Real-time Scan-Matching Using L_0-norm Minimization Under Dynamic Crowded Environments

Yusuke Hieida[1], Tsuyoshi Suenaga[1], Kentaro Takemura[1], Jun Takamatsu[1] and Tsukasa Ogasawara[1]

***Abstract*— We propose real-time scan-matching based on L_0-norm minimization under dynamic crowded environment. The prior scan-matching methods are based on L_2-norm minimization, because the measurement noise follows the normal distribution in static environments. This assumption is unfortunately broken in dynamic crowded environments.**

We propose to use the idea of Locality Sensitive Hashing (LSH) to accelerate the L_0-norm minimization, which usually is a time-consuming process. The LSH customized for our issue reduces the calculation time even in the worst cases. The experimental results demonstrate the effectiveness of the proposed method compared with standard L_2-norm minimization and its robust version with M-estimator.

I. Introduction

It is very demanded for an autonomous robot to move under unknown environments [1]. *Scan-matching* estimates robot's displacement by aligning time-series measurements. Concatenation of displacement and the aligned measurement generate robot's trajectory and the map respectively, while may suffer from accumulation of alignment errors. Iterative Closest Point (ICP) method [2] and particle filter [3], [4] improve the performance under static environments [5].

However, the assumption valid for static environments is broken in real-world environments. Under dynamic crowded environments, the accuracy of the alignment deteriorates because both static (referred to as *inliers*) and moving objects (referred to as *outliers*) are rigidly aligned, resulting in poor performance of the prior methods (Fig. 1). To robustify outliers in the alignment is inevitable under dynamic environments.

A. Related work

There are two types of approaches for dynamic environments. One approach explicitly detects inliers/outliers by feature extraction, tracking and so on. The other approach gradually or simultaneously estimates the likelihood of outliers and decreases their effect during the alignment.

In the first approaches, Wolf and Sukhatme [6] proposed to use only landmarks, which tend to be static, as inliers. Examples of landmarks are wall planes and corners. Wang *et al*. [7] propose to interleave object tracking based on motion detection. Hähnel *et al*. [8] also propose to use object tracking based on the sample joint probabilistic data association filter. Rodriguez-Losada and Minguez [9] prove that the possible displacement to satisfy correspondence of one point between two frames is helix and detect the outliers by using the distance to the helix. The performance of these methods deeply depends on the detection of inliers/outliers.

In the second approaches, Hähnel *et al*. propose to use the expectation-maximization (EM) algorithm [10]. The E-step evaluates likelihood of outliers and the M-step aligns measurements with weighting according to the likelihood. Ramos *et al*. [11] propose to use the conditional random field (CRF) to stochastically estimate data association and outliers. Further, Ven *et al*. [12] estimate moving object and motion as well as data association. Since these methods need to optimize the function with large number of parameters, it is difficult to achieve real-time operation.

Viewing from the outlier detection, use of robust statistics, such as M-estimator [13], is one of the solutions. There are several methods that use M-estimator for scan matching-based alignment [14], [15]. Although the optimization of the M-estimator is simpler and thus faster than the second approaches, it may also lack of inappropriate convergence.

B. Proposed method

We propose real-time scan-matching that suits adapted to dynamic environments. We use a common real-time LIDAR sensor, which measures depths only on the cross-sectional plane. Thus, we assume that the ground is flat and the measuring cross-section is parallel to the ground. We believe that the proposed method can be extended to its 3-D version.

The novelty of the proposed system is to use L_0-norm being that the prior systems use L_2-norm. Although optimization of the L_0-norm tends to be time-consuming, we propose to use the Locality Sensitive Hashing (LSH) [16] to make the proposed method suitable for real-time.

The Contributions of this paper are twofold:

- We experimentally prove that the effectiveness of the L_0-norm for scan-matching under dynamic environments. Note that such norm is often employed in other applications, such as face recognition [17], image inpainting [18], and denoising [19].
- We propose to accelerate the L_0-norm calculation with approximation using the LSH [16]. Unlike the L_2-norm calculation, we only need to decide if the other points exist inside the pre-defined radius and it is not necessary to consider their point ID. These aspects stabilize the calculation time even in the worst cases and reduce memory consumption by removing the point ID information.

[1]They are with Graduate School of Information Science, Nara Institute of Science and Technology, Japan {yusuke-h, tsuyo-s, kenta-ta, j-taka, ogasawar} at is.naist.jp

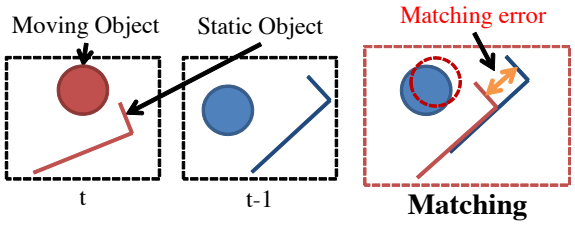

Fig. 1. Erroneous estimation of displacement due to dynamic environment. The circular object moves rightward from time $t-1$ (middle) to time t (left), while the L-shape object is fixed. Alignment only using the L-shape object outputs the correct displacement. But the prior scan-matching methods diffuse matching errors uniformly in the space, resulting in erroneously estimating the displacement.

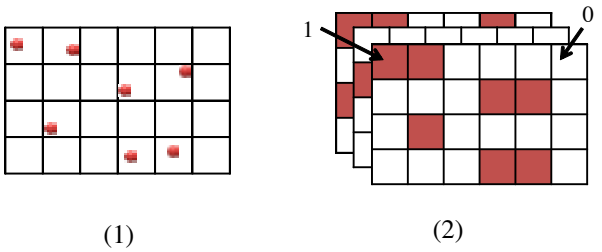

Fig. 2. Several boolean-array tables are generated by the LSH. Each bin represents the existence of r-near neighbors and thus the existence is decided by accessing the corresponding bin in $O(1)$ time.

II. Preliminary

Consider two point sets, $\{\mathbf{p}_i\}$ and $\{\mathbf{q}_j\}$, which are measurements of the same environment, but they have different coordinates, *i.e.*, measurements from different positions. Robot's displacement is estimated by aligning these two sets.

In scan-matching scenario, displacement is estimated by minimizing the evaluation function $E(\mathbf{R},\mathbf{t})$ in Eq. (1) [1].

$$E(\mathbf{R},\mathbf{t}) = \sum_{i=1}^{n} f(\mathbf{R}\mathbf{p}_i + \mathbf{t}, \{\mathbf{q}_j\}) = \sum_{i=1}^{n} f(\mathbf{p}'_i, \{\mathbf{q}_j\}), \quad (1)$$

where n is the number of the points $\{\mathbf{p}_i\}$, $\mathbf{p}'_i \stackrel{\text{def}}{=} \mathbf{R}\mathbf{p}_i + \mathbf{t}$, a 2×2 matrix $\mathbf{R}$ represents the orientation and a 2-D vector $\mathbf{t}$ represents the translation in robot's planer displacement. The function f defines the distance between the point $\mathbf{p}'_i$ and the measurement $\{\mathbf{q}_j\}$. In prior methods [2], the function f is Euclidean distance between $\mathbf{p}'_i$ and the closest point $\mathbf{q}_c$ of the measurement, as $f(\mathbf{p}'_i, \{\mathbf{q}_j\}) = ||\mathbf{p}'_i - \mathbf{q}_c||^2$.

III. Scan-matching based on L_0-norm

A. Definition of L_0-norm

Given two sets of points, $\{\mathbf{p}_i\}$ and $\{\mathbf{q}_j\}$, the evaluation function $E(\mathbf{R},\mathbf{t})$ based on L_0-norm is similarly defined as Eq. (1), but the definition of the function f is different, such as

$$f(\mathbf{p}'_i, \{\mathbf{q}_j\}) = \begin{cases} 0 & (\exists j, ||\mathbf{p}'_i - \mathbf{q}_j|| \le \epsilon) \\ 1 & (\text{otherwise}) \end{cases}. \quad (2)$$

The distance threshold ϵ is a constant real number, which is decided based on the accuracy of the measurement. The evaluation function counts the points which do not have any points near the distance less than ϵ. Note that calculation of the L_0-norm does not require the explicit point correspondences, just to decide if the other points exist inside the radius ϵ. We refer to these points as *r-near neighbors* following the terminology in [16].

B. Acceleration by Locality Sensitive Hashing

We employ the Locality Sensitive Hashing (LSH) [16], whose calculation time is $O(1)$. The LSH limits the search space using the hash function, whose values of two proximity points tend to be the same. In the LSH, only the points with similar hash values are considered. Using multiple hash functions reduces the tendency to failure in the search. Concretely, the hash function is defined as

$$h(\mathbf{x}) = \left\lfloor \frac{\mathbf{a}\cdot\mathbf{x} + b}{w} \right\rfloor, \quad (3)$$

where the symbol $\lfloor\ \rfloor$ means floor operation, $\mathbf{x}$ is the data point, w is the width of the hash bin and the parameters $\mathbf{a}$ and b are randomly chosen by p-degree stable distribution and uniform distribution from 0 to w, respectively. We only consider the projection of x- and y-axes as the vector $\mathbf{a}$, *e.g.*, $(a_x, 0)$ and $(0, a_y)$, and use them by concatenating x- and y-axis projection LSH as shown in Fig. 2. The existence of r-near neighbor is searched by accessing the bin of the table several times (at most, number of tables).

Although the LSH is usually used for nearest neighbor search, the LSH in r-near neighbor search has two more advantages. In the nearest neighbor search, when all the searched points $\{\mathbf{q}_j\}$ have different hash values, it is necessary to continue searching the points whose values are near to the target value. However in r-near neighbor search, the calculation is just terminated and we conclude that no r-near neighbor exists. L_0-norm does not consider the position or ID of the r-near neighbor, and depends only on the existence.

IV. Minimization by importance sampling

The approximate robot's displacement is obtained from odometry or control inputs. Thus, we use the sampling-based optimization method considering importance of searched region. In strict sense, minimization of L_0 norm is equivalent to combinatorial optimization. In this sense, using the method in [20] is alternative and future work.

We minimize the evaluation function using importance sampling and coarse-to-fine search as shown in Fig. 3:

1) randomly generate n_1 locations (referred to as sample-A) based on odometry or control inputs
2) calculate the importance of each sample by Eq. (4).
$$\exp\left(\frac{m - E(R,\mathbf{t})}{k}\right). \quad (4)$$
The parameter k controls the degree of the importance with respect to the evaluation function.
3) select n_2 locations (referred to as sample-B) from sample-A following their weights.

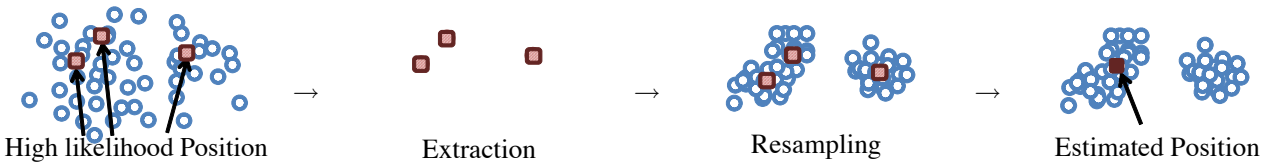

Fig. 3. Minimization by importance sampling and coarse-to-fine search. By gradually changing the distribution σ of sampling range, the samples converge on the minimum in the L_0-norm.

(a) LIDAR: SICK LMS100 (b) Mobile robot: EMC-230

Fig. 4. Equipments used in this experiment

TABLE I
SPECIFICATION OF SICK LMS100

Viewing angle	270 [deg]
Angular resolution	0.5 [deg]
# of points in each frame	540
Accuracy in depth	1.2 [cm]
Maximum depth	20 [m]
Frequency	30 [Hz]

4) randomly generate n_3 locations by normal distribution with variance $(\sigma_x, \sigma_y, \sigma_\theta)$ around from sample-B. $n_2 \times n_3$ locations are sampled in total.
5) repeat 2) to 4) in several times, while reducing variances.

V. EXPERIMENTS

A. Experimental setup

We used the LIDAR, SICK *LMS100* (Fig. 4 (a)), and a wheelchair, *EMC-230* made by Imasen Engineering Corporation as the mobile robot (Fig. 4 (b)). This LIDAR measures uniformly along the angle direction and thus the measured points become sparser as the depth increases. Considering the calculation time and the estimation accuracy, the measured points $\{\mathbf{p}_i\}$ are segmented and thinned out so that the points are distributed uniformly in the space. On the other hand, in the measured points $\{\mathbf{q}_j\}$, additional points are inserted as all the intervals of neighbors are less than the threshold ϵ in Eq. (2). We set ϵ to 1 [cm] based on the accuracy of the LIDAR used in this experiment (see Table I).

We conducted three types of experiments. The first experiment verifies the effectiveness of the L_0-norm in outliers compared with simple ICP, ICP with thresholding, and ICP with M-estimator, which are most related to the proposed method. Note that first approaches described in Section I-A use such methods after detecting outliers. The second experiment verifies the effectiveness of the LSH with respect to the calculation time and accuracy. The third experiment verifies the applicability of the proposed method through actual use. The experimental environment is mainly the inside of a building of our campus.

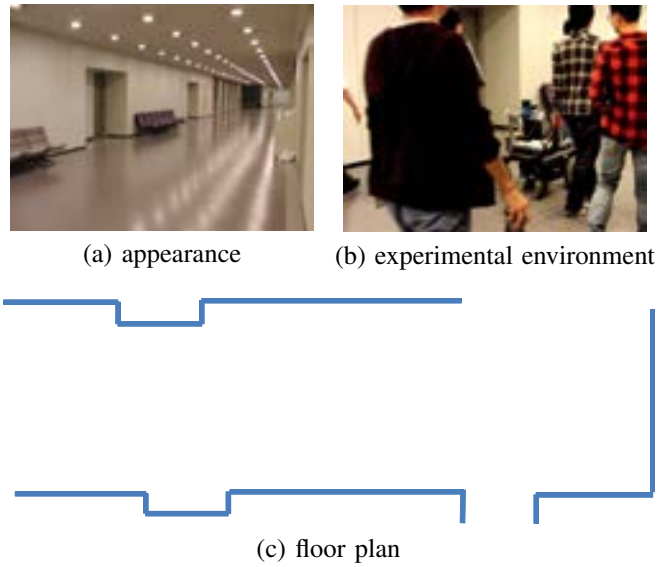

(a) appearance (b) experimental environment

(c) floor plan

Fig. 5. Experimental environment. (a) appearance of the inside of the building. (b) actual experimental environment crowded by people. (c) floor plan of the environment.

B. Verification of effectiveness of L_0-norm

Figure 5 shows the experimental environment which is about 5 [m] in width and 20 [m] in depth. About 25 people are moving toward the robot within the environment. The robot measures the environment while fixed. Thus, the estimated robot displacement (x, y, θ) should be always zero, where x, y, and θ are the translation along the x- and y-axes and the orientation, respectively.

To verify the effectiveness without considering the initial guess, we optimize all of the functions by brute-force search, where the ranges of x, y, and θ are $[-5\ \text{[cm]}, 5\ \text{[cm]})$, $[-5\ \text{[cm]}, 5\ \text{[cm]})$, and $[-0.3\ \text{[rad]}, 0.3\ \text{[rad]})$ and sampled uniformly at 0.5 [cm], 0.5 [cm], and 0.01 [rad] ($\fallingdotseq$ 0.57 [deg]), respectively. There are 24000 samples in total.

In ICP with thresholding, we ignore some ratio of the further corresponding data as outliers. We employ the Cauchy and the Biweight function as M-estimator $\rho(d)$ and use $\rho(f(\mathbf{R}\mathbf{p}_i+\mathbf{t}, \{\mathbf{q}_j\}))$ in place of $f(\mathbf{R}\mathbf{p}_i+\mathbf{t}, \{\mathbf{q}_j\})$ in Eq. (1). The Cauchy function is defined as Eq. (5) and is often used (*e.g.* [14], [15]):

$$\rho(d) = \frac{C^2}{2} \log\left(1 + \left(\frac{d}{C}\right)^2\right), \tag{5}$$

TABLE II

MSE OF THE ESTIMATED LOCALIZATION: L_2-NORM (SIMILE ICP), THRESHOLD (IGNORE SOME RATIO OF THE FURTHER CORRESPONDING DATA AS OUTLIERS), M-ESTIMATOR (CAUCHY AND BIWEIGHT FUNCTIONS) AND L_0-NORM

Method	MSE (x [cm], y [cm], ϕ [rad])
L_2-norm	(3.37, 2.08, 0.016)
Threshold (30 percents)	(1.17, 0.033, 0)
Threshold (50 percents)	(0.19, 0.004, 0)
Cauchy	(1.33, 0.013, 0)
Biweight	(0.13, 0.002, 0)
L_0-norm	(0.42, 0.015, 0)

TABLE III

COMPARISON AMONG THREE KINDS OF r-NEAR NEIGHBOR SEARCH: SIMPLE METHOD, KD-TREE METHOD, AND LSH. THE LSH OPERATES AT HIGH SPEED, BUT SACRIFICES THE ACCURACY.

method	time [s]	# of localizations per second	RMSE of the L_0-norm
simple	126	190	-
kd-tree	24	1000	-
LSH	5.4	4436	14.4

where C is a positive real value. The Biweight function is defined as Eq. (6) and completely removes the effect of the outliers (shape of the function is flat in the region $|e| \geq 0.01$) similar to the proposed L_0-norm.

$$\rho(d) = \begin{cases} \frac{B^2}{2} & (d \geq B) \\ \frac{B^2}{2}\left(1 - \left(1 - \left(\frac{d}{B}\right)^2\right)^3\right) & (d < B) \end{cases}, \quad (6)$$

where B is a positive real value. Both values, B and C, are set to 1 [cm] considering the sensor's accuracy.

Since the estimated displacement should be zero as described before, we quantitatively compare them using the mean square error (MSE) of the displacement. Table II shows the results. The estimation by the L_0-norm, L_2-norm with higher threshold, and the Biweight function are similar and better than the others, because sensor accuracy is 1.2 [cm]. This result demonstrates the effectiveness of the L_0-norm, which regards the point outside of the pre-defined radius as outliers. The Biweight function and ICP with higher threshold have a similar characteristic and thus achieves a better performance. But this means that these three methods have the same disadvantages with respect to the convergence. Note that distance used as threshold in ICP with thresholding is decided in each brute-force step.

Figures 6 to 9 show the maps estimated by these methods, respectively. Each map is constructed by overlaying all the measurements according to the estimated displacement. The red line shows robot's displacement, which should not appear. The outer boundary shows the static walls of the building (See Fig. 5 (c)), while the inner points indicate moving people. If the map is appropriately estimated, the outer boundary should be aligned without blurring. These figures also demonstrate the effectiveness of the L_0-norm.

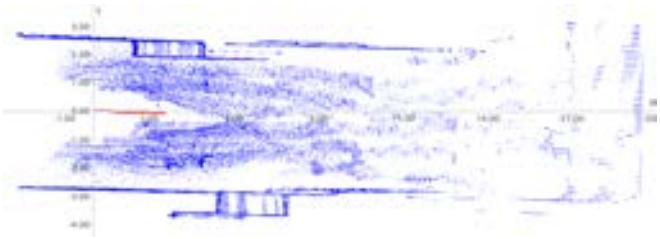

Fig. 6. The map estimated by the L_2-norm minimization with 30 percent threshold. The red line indicates robot's displacement and the blue points indicate measured points on the global coordinates. Since the robot is fixed, the red line should not appear. Since the blue points on the outer boundary corresponds to the wall of the building (Fig. 5 (c)), they should not be blurred.

Fig. 7. The map estimated by the Cauchy function

C. Verification of effectiveness of LSH

We compare the proposed LSH acceleration with the simple method and the kd-tree method [22]. The computer to employ is composed of Intel *Core2Duo T7500* (Clock speed: 2.2 [GHz]) and 2 [GB] memory. We conducted this experiment with the same configuration of the previous experiment, but the robot moved.

Table III shows the average calculation time for the brute-force search (24000 times of calculation), number of L_0-norm calculations per second and the root mean square error (RMSE) of the calculated L_0-norm; the simple and kd-tree methods always output correct answers, but the LSH method does not. In calculation time, the LSH method is about five times faster than the kd-tree method, but sacrifices the accuracy; RMSE of the L_0-norm is 14.4, while the average of the norms is 280.03.

To evaluate the degeneration caused by the approximation of the L_0 norm calculation, we actually construct the map using the LSH method. Figure 10 shows the map which the RBPF-SLAM method [21] estimates from measurement of the static environment and we regard it as ground truth. Figure 11 shows the map which the LSH method estimates from measurement of the same but dynamic environment. Despite the approximation, the estimated map is acceptable in visual inspection.

D. Verification in Actual Use

We actually estimate the map using the proposed method, which includes the LSH method and minimization by the importance sampling. The localization at each frame is performed at about 5 [fps] on the same computer as that of Section V-C. The parameters are: n_1 = 300, n_2 = 20, n_3 = 15, k = 20.0. Steps 2) to 4) are repeated twice,

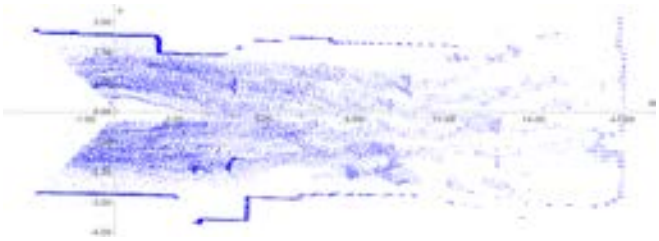

Fig. 8. The map estimated by the Biweight function

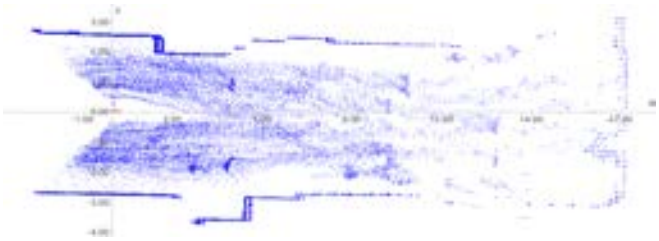

Fig. 9. The map estimated by the L_0-norm minimization

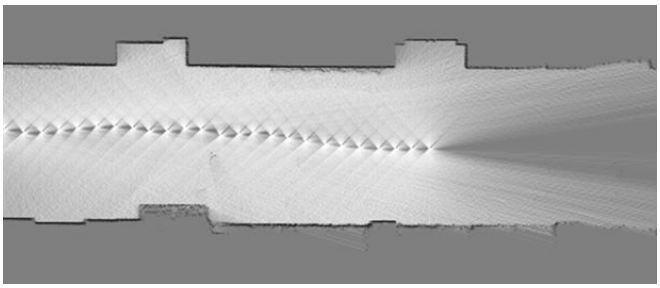

Fig. 10. The map estimated by the RBPF-SLAM method [21] under the environment without moving objects.

Fig. 11. The map estimated by L_0-norm under the same environment as Fig. 10, but including moving objects.

and $(\sigma_x, \sigma_y, \sigma_\theta) = (0.03, 0.03, 0.025)$ at the first time and $(\sigma_x, \sigma_y, \sigma_\theta) = (0.01, 0.01, 0.01)$ at the second time.

In the first experiment, the size of the experimental environment is about 50 [m] $\times$ 30 [m]. About 25 people are moving around the robot as outliers as shown in Fig. 12. 300 frames of measurements are used. Figure 13 shows the estimated map. Figure 14 shows the occupancy grid map obtained from the estimation results using the open SLAM software *MRPT* [1]. We overlay the floor plan of this building to evaluate the accuracy.

Figure 15 shows the estimated map in the second experiment, which includes both indoor and outdoor measurements. The size of the experimental environment is about 100 [m] $\times$ 60 [m]. 700 frames of measurements are used. To evaluate the accuracy of the map, we overlay the aerial photograph downloaded from the Google maps[2].

E. Discussion

Both the L_0-norm, ICP with higher threshold, and the Biweight function have similar advantages and disadvantages. Unlike the other two methods, by ignoring the distance and ID of the r-near neighbor in the LSH, the L_0-norm calculation is accelerated. Despite ignoring them, the localization accuracy is surprisingly maintained as shown in the experiments. Note that better results obtained by these three methods strongly support the plausibility of using the L_0-norm.

VI. Conclusion

In this paper, we proposed real-time scan-matching for dynamic environments, which works at about 5 [fps] on Intel Core2Duo T7500 (Clock speed: 2.2 [GHz]) with 2 [GB] memory. The proposed method uses L_0-norm, not L_2-norm, for alignment. First, we proved the robustness of the L_0-norm to outliers through actual use.

Next, we proposed to accelerate r-near neighbor search by the LSH technique. Unlike the nearest neighbor search, we only need to determine if r-near neighbors exist and it is not necessary to consider the IDs of the neighbors. These aspects do not affect the calculation time even in the worst cases and reduce memory consumption by removing the point ID information.

The proposed method estimates the displacement only from two subsequent measurements. Generally, scan-matching suffers from accumulation of the estimation errors. *Loop-closing* technique [23] is one of the solutions.

[1] http://www.mrpt.org

[2] http://maps.google.com

References

[1] S. Thrun, W. Burgard, and D. Fox, *Probabilistic robotics*. The MIT Press, 2005.

[2] P. J. Besl and N. D. McKay, "A method for registration of 3-D shapes," *IEEE Trans. on Patt. Anal. and Mach. Intell.*, vol. 14, no. 2, pp. 239–256, 1992.

[3] M. Isard and A. Blake, "CONDENSATION - conditional density propagation for vision tracking," *Int. J. of Computer Vision*, vol. 29, no. 1, pp. 5–28, 1998.

[4] S. Godsill, A. Doucet, and M. West, "Maximum a posteriori sequence estimation using monte carlo particle filters," *Ann. Inst. Statist. Math.*, vol. 53, pp. 82–96, 2001.

[5] S. Thrun, "Simultaneous mapping and localization with sparse extended information filters: Theory and initial results," *Algorithmic Foundations of Robotics V*, vol. 7, pp. 363–380, 2003.

[6] D. F. Wolf and G. S. Sukhatme, "Mobile robot simultaneous localization and mapping in dynamic environments," *Autonomous Robots*, vol. 19, no. 1, pp. 53–65, 2005.

[7] C. C. Wang, C. Thorpe, and S. Thrun, "Online simultaneous localization and mapping with detection and tracking of moving objects: Theory and results from a ground vehicle in crowded urban areas," in *Proc. of Int. Conf. on Robotics and Automation (ICRA)*, 2003.

[8] D. Hähnel, D. Schulz, and W. Burgard, "Map building with mobile robots in populated environment," in *Proc. of Int. Conf. on Intelligent Robots and Systems (IROS)*, 2002.

Fig. 12. Snapshots of images obtained from digital camera (left column) and SICK LMS100 (right column) installed in the robot.

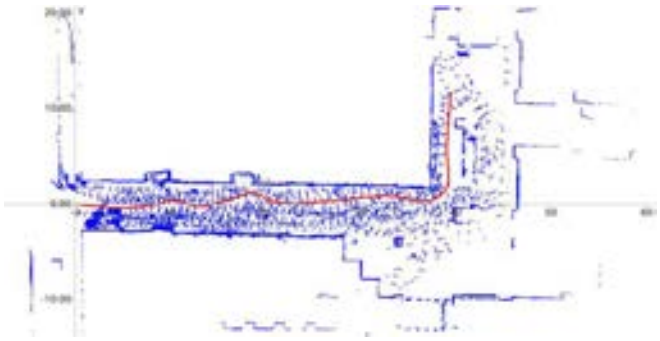

Fig. 13. The map estimated by the L_0-norm minimization

[9] D. Rodriguez-Losada and J. Minguez, "Improved data association for icp-based scan matching in noisy and dynamic environments," in *Proc. of Int. Conf. on Robotics and Automation (ICRA)*, 2007.

[10] D. Hähnel, R. Triebel, W. Burgard, and S. Thrun, "Map building with moblile robots in dynamic environments," in *Proc. of Int. Conf. on Robotics and Automation (ICRA)*, 2003.

[11] F. Ramos, D. Fox, and H. Durrant-Whyte, "Crf-matching: Conditional random fields for feature-based scan matching," in *RSS*, 2007.

[12] J. van de Ven, F. Ramos, and G. D. Tipaldi, "An integrated probabilistic model for scan-matching, moving object detection and motion estimation," in *ICRA*, 2010.

[13] P. J. Huber, *Robust statistics*. Wiley-Interscience, 1981.

[14] M. D. Wheeler and K. Ikeuchi, "Sensor modeling, probabilistic hypothesis generation and robust localization for object recognition," *IEEE Trans. on Patt. Anal. and Mach. Intell.*, vol. 17, no. 3, pp. 252–265, 1995.

Fig. 14. The occupancy grid map obtained by the open SLAM software *MRPT* and the proposed method. We overlay the floor plan of this building to evaluate the accuracy.

Fig. 15. The map estimated by the proposed method. We overlay the corresponding aerial photograph from the *Google Maps* to evaluate the accuracy.

[15] K. Kawamura, K. Hasegawa, Y. Someya, Y. Sato, and K. Ikeuchi, "Robust localization for 3D object recognition using local EGI and 3D template matching with m-estimators," in *Proc. of Int. Conf. on Robotics and Automation (ICRA)*, 2000.

[16] A. Andoni, M. Datar, N. Immorlica, P. Indyk, and V. Mirrokni, *Locality-sensitive hashing scheme based on p-stable distributions, nearest neighbor methods in learning and vision*. MIT Press, 2006.

[17] J. Wright, A. Yang, A. Ganesh, S. Sastry, and Y. Ma, "Robust face recognition via sparse representation," *IEEE Trans. on Patt. Anal. and Mach. Intell.*, vol. 31, no. 2, pp. 210–227, 2009.

[18] L. Mancera and J. Portilla, "L0-norm-based sparse representation through alternate projections," in *Proc. of Int. Conf. on Image Processing (ICIP)*, 2006.

[19] H. Ji, C. Liu, Z. Shen, and Y. Xu, "Robust video denoising using low rank matrix completion," in *Proc. of Int. Conf. on Comp. Vis. and Patt. Anal. (CVPR)*, 2010.

[20] E. B. Olson, "Real-time correlative scan matching," in *Proc. of Int. Conf. on Robotics and Automation (ICRA)*, 2009.

[21] G. Grisetti, C. Stachniss, and W. Burgard, "Improved techniques for grid mapping with rao-blackwellized particle filters," *IEEE Transactions on Robotics*, vol. 23, pp. 34–46, 2007.

[22] J. L. Bentley, "Multidimensional binary search trees used for associative searching," *ACM Commun.*, vol. 18, pp. 509–517, 1975. [Online]. Available: http://doi.acm.org/10.1145/361002.361007

[23] C. Stachniss and W. Burgard, "Exploration with active loop-closing for FastSLAM," in *Proc. of Int. Conf. on Intelligent Robots and Systems (IROS)*, 2004.